

## Article

# The Effects of Unpowered Soft Exoskeletons on Preferred Gait Features and Resonant Walking

Zhengyan Zhang <sup>1</sup>, Houcheng Wang <sup>1</sup> , Shijie Guo <sup>1,\*</sup>, Jing Wang <sup>2</sup>, Yungang Zhao <sup>2</sup> and Qiang Tian <sup>2</sup>

<sup>1</sup> School of Mechanical Engineering, Hebei University of Technology, Tianjin 300401, China; zzy@hebut.edu.cn (Z.Z.); rijikarrd@sina.com (H.W.)

<sup>2</sup> Tianjin Key Laboratory of Exercise Physiology and Sports Medicine, Institute of Exercise and Health, Tianjin University of Sport, Tianjin 301617, China; xiaojing111213@126.com (J.W.); yungang.zhao@tjus.edu.cn (Y.Z.); jackietian2008@126.com (Q.T.)

\* Correspondence: guoshijie@hebut.edu.cn

**Abstract:** Resonant walking with preferred gait features is a self-optimized consequence of long-term human locomotion. Minimal energy expenditure can be achieved in this resonant condition. This unpowered multi-joint soft exoskeleton is designed to test whether: (1) there is an obvious improvement in preferred speed and other gait features; (2) resonant walking still exists with exoskeleton assistance. Healthy participants (N = 7) were asked to perform the following trials: (1) walking at 1.25 m/s without assistance (normal condition); (2) walking at 1.25 m/s with assistance (general condition); (3) walking at preferred speed with assistance (preferred condition); (4) walking at the speed in trial (3) without assistance (comparison condition). Participants walked at the preferred frequency and  $\pm 10\%$  of it. An average 21% increase in preferred speed was observed. The U-shaped oxygen consumption and lower limb muscle activity curve with the minimum at preferred frequency indicated that the resonant condition existed under the preferred condition. Average metabolic reductions of 4.53% and 7.65% were found in the preferred condition compared to the general and comparison condition, respectively. These results demonstrate that the resonant condition in assisted walking could benefit energy expenditure and provide a new perspective for exoskeleton design and evaluation.

**Keywords:** resonant walking; preferred gait features; unpowered soft exoskeletons; oxygen consumption; lower limb muscle activity



**Citation:** Zhang, Z.; Wang, H.; Guo, S.; Wang, J.; Zhao, Y.; Tian, Q. The Effects of Unpowered Soft Exoskeletons on Preferred Gait Features and Resonant Walking. *Machines* **2022**, *10*, 585. <https://doi.org/10.3390/machines10070585>

Academic Editor: Yanjie Wang

Received: 13 May 2022

Accepted: 11 July 2022

Published: 18 July 2022

**Publisher's Note:** MDPI stays neutral with regard to jurisdictional claims in published maps and institutional affiliations.



**Copyright:** © 2022 by the authors. Licensee MDPI, Basel, Switzerland. This article is an open access article distributed under the terms and conditions of the Creative Commons Attribution (CC BY) license (<https://creativecommons.org/licenses/by/4.0/>).

## 1. Introduction

Exoskeletons can be divided into three types: rehabilitation exoskeleton, assisting exoskeleton and load-bearing exoskeleton [1,2]. Rehabilitation exoskeletons are mainly used to provide recovery training for people with movement disorders such as stroke patients. Assisting exoskeletons are mainly used for healthy people with declining body functions or the elderly and patients in late rehabilitation. They mainly provide the human body with motion assistance for daily activities, such as level ground walking. Load-bearing exoskeletons are mainly used to improve the user's motor function during weight-bearing activities. Understandably, there has been much interest from the military, where the technology could enhance the performance of soldiers in the battlefield [3]. In addition to whether there is an actuator, the exoskeleton can also be divided into rigid and soft ones according to the structure. The rigid structure is able to transmit large torques, but there are problems such as large volume, heavy mass and joint axis alignment; soft exoskeletons are generally referred to as devices that are made of flexible materials, and their distal end is lightweight and easy to carry and use. The powered rigid exoskeleton can accomplish the above three tasks, but it is not suitable for daily use due to its large volume, heavy mass and short battery life. The powered soft exoskeleton is suitable for daily use as it is light in weight and easy to carry, but its soft structure also means it lacks the ability

to bear weight, so it is mainly used for rehabilitation and walking assistance in daily life. Unpowered exoskeletons are also divided into rigid ones and soft ones. The removing of actuator units reduces the mass and volume to make it more suitable for daily use, but this will also lead to lack of assistance ability. As a result, unpowered exoskeletons are mostly used in walking assistance for the reduction of fatigue during daily activities.

Unpowered and soft exoskeletons have been evidenced to improve overall walking efficiency and performance [4–8]. Elastic elements are used to passively store and return energy as one of the main mechanisms in existing unpowered exoskeletons, which are inspired by the deformation of passive structures such as ligaments and tendons during periodic walking [9–11]. Paralleled with the elastic tissues, elastic elements are able to simulate and replace part of their functions, hence the energy savings. During each gait cycle, the energy stored in previous periods will be returned in subsequent movements to propel the body forward [12–17]. As these exoskeletons primarily save energy through the storage and release of elastic elements, the main focus is the spring stiffness (torque profile), the design of devices [18,19] and the assistance timing [6]. When evaluating the assisting ability of exoskeletons, the speed of treadmills was always set in the range of ordinary people's comfortable speed (around 1.25 m/s) to simulate the daily walking condition. In addition, a fix-speed treadmill is useful to constrain speed and isolate the effects of exoskeleton assistance on gait features other than speed.

For unpowered devices, the interaction between gait features and assistance magnitude could be complex, as it should be actuated by users, which will influence the characteristics of human walking. At a certain speed, metabolic rate reaches a minimum at moderate stiffness and then increases rapidly with increasing or decreasing stiffness, with a U-shaped curve. What is more, under the same assisting parameter setting and experimental condition, the metabolic reduction of different subjects varies greatly, and some of them even rise. These results indicate that the effect of the exoskeleton on walking is obviously closely related to the speed and the physical parameters of the individual subjects, and these aspects will greatly affect the exoskeleton assistance. However, previous studies have not paid much attention to the problems above. While for unpowered devices, In the research of Collins [20], participants chose a higher preferred speed with speed-optimized torque obtained from human-in-the-loop optimization rather than torque optimized for energy consumption and normal shoes. This result demonstrated that exoskeleton assistance does have an impact on gait features and can significantly improve the preferred walking speed.

Resonant walking, which appears under preferred gait features, is regarded as the optimal result of human walking, and its periodic behavior could be simulated by the force-driven harmonic oscillator (FDHO) [21,22]. Due to the existence of damping, a periodic forcing function is required to maintain the oscillation of the FDHO. Thus, the minimal force can be reached when its frequency equals the natural frequency of the FDHO. For human walking, lower force (muscle activity) results in a decreased need for oxygen, hence a minimization at resonant frequency. Self-selected preferred speed and frequency have been proven to be almost indistinguishable from the resonant ones. U-shaped oxygen consumption and muscle activity curves were observed with the minimum at the preferred and resonant frequency, increasing away from the preferred frequency [23–25], which also means the frequency range for achieving better metabolic performance is flexible. Local dynamic stability is also an important part of resonant walking, such as maintaining the highest stability of the head at the preferred frequency [24].

Several models have been built to describe resonant walking. Holt has proposed a hybrid mass-spring pendulum model for the swing phase and an escapement-driven, inverted pendulum with a spring model (EDIPS) with viscous damping for the stance phase, based on the force-driven harmonic oscillator [26–28]. Park tuned a model of bipedal walking with damped compliant legs to match human GRFs(ground reaction forces)s at different gait speeds and performed a series of studies based on the bipedal spring-mass model by Geyer [29–34]. The correlation between leg stiffness and center of mass (COM) oscillation behavior during the single-support phase was evaluated by

comparing the duration of the damped compliant leg to the duration of the single support phase. The high correlation indicated that COM oscillation behavior takes advantage of the resonance characteristics of leg stiffness during the single support phase, and results also suggested that the leg stiffness increases with speed and load. Contrary to the conventional assumption in gait mechanics that a minimal change in COM excursion can reduce energy cost, previous studies have mentioned that a bouncy gait is more energy-efficient than a flat trajectory [31,35]. This observed bouncy behavior results from the resonant mechanics [30] and has already been used in some assistive devices [36].

As elastic elements are actuated by users during assisted walking, they actually become a part of the human body in the specific period when stretched. At this time, the body and device can be regarded as a new “person” with different global lower limb stiffness. According to a previous study, the preferred step frequency changes with lower limb stiffness and the preferred speed increases with exoskeleton assistance and leg stiffness, thus leading to a new gait feature. It is believed that resonant walking will occur under the new preferred gait feature, and the changes of preferred gait features should be taken into consideration for a further global optimization of assisted walking, as shown in Figure 1.

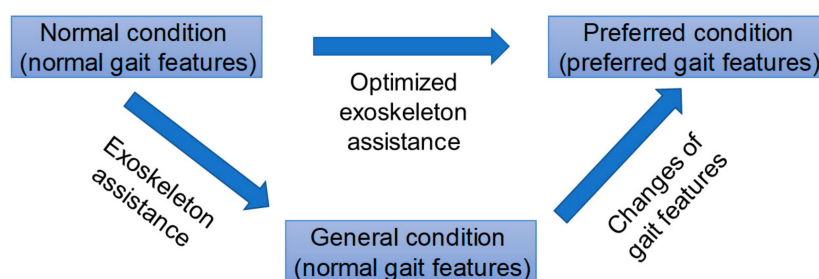


**Figure 1.** Schematic diagram of assisted walking when considering the changes of the gait feature.

The main purpose of this study was to investigate the questions as follows: whether (1) unpowered exoskeletons can change the preferred speed and gait features; (2) resonant walking occurs under different gait features with exoskeleton assistance. Finally, the net metabolic rate under different conditions was analyzed to evaluate the effect of resonant walking with assistance on walking efficiency. To conduct this research, a multi-joint unpowered soft exoskeleton was designed with two assistance paths, the anterior and posterior of the body. Details of the exoskeleton will be described in the next section.

## 2. Materials and Methods

### 2.1. Design of the Exoskeleton

The exoskeleton was made of commercially available resistance bands (TheraBand Professional Latex Resistance Band Gold, TheraBand, Akron, OH, USA), nylon fabric and waist bands, which led to a lightweight device. The three main parts (waistband, hip-ankle assistance path and hip-knee assistance path) and the deformation of springs are shown in Figure 2. The resistance bands were cut into segments with a length of 18 cm (with two 5 cm hook and loop fasteners at each end of both sides) and placed in front and behind the body bilaterally. The waist band is used for an anchor on the upper body to resist the tension of elastic bands. Leg straps 1 are used to connect the anterior spring and foot attachment, while leg straps 2 are used to connect the posterior springs and calf attachment. The connection between the elastic bands and other straps or bands is hook and loop. Before the experiment, elastic bands were first pretensioned by 1.5 cm (initial length) to obtain a preload.

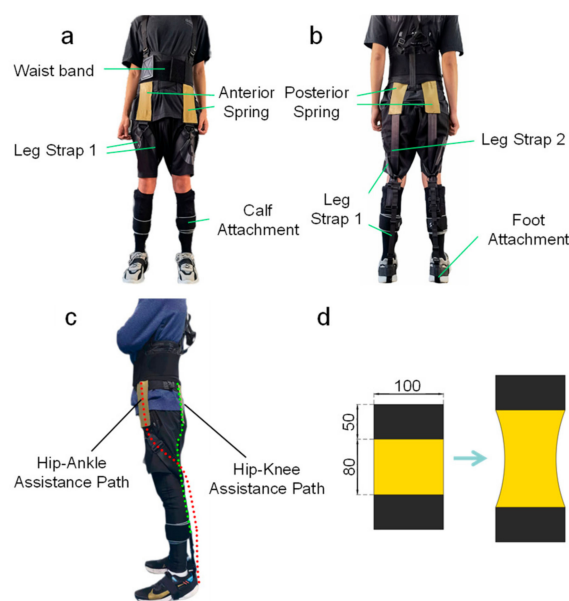


**Figure 2.** Overview of the soft exoskeleton. (a) Front and (b) rear view of the device; schematic diagram of the hip-ankle assistance path and the hip-knee assistance path; (c) schematic diagram of the geometry of the elastic elements placed anteriorly and posteriorly across the hip; (d) dimensions are in millimeters.

The anterior path is used to absorb energy in the stance phase and return when push-off occurs to help plantarflexion and hip flexion. The posterior path is used to absorb energy in the swing phase and return it in the following movements in order to transform the negative power from the knee joint to the hip joint to help hip flexion.

The energy storage and return phase of both anterior and posterior springs are described here (see Figure 3). For the hip-knee assistance path, the elastic energy is stored from the late swing phase and then released in the coming movements. While for the hip-ankle assistance path, the elastic energy is stored from early mid-stance to heel-off, and then released gradually after heel-off. The details of the assistance are not presented here as this is not the main focus of this article.

## 2.2. Experimental Setup

Participants walked on a treadmill (h/p/cosmos pulsar 4.0, h/p/cosmos, Traunstein, Germany) with a heart rate belt to record heart rates and a gas analysis machine (MetaMax 3B-R2, Cortex, Leipzig, Germany) to measure the oxygen uptake and carbon dioxide exhalation. Electrical muscle activity was measured with 12 wireless EMG (ElectroMyoGraphy) transmitters (Noraxon Ultium EMG, Noraxon, Scottsdale, AZ, USA) at 2000 Hz (Figure 4). The signal was filtered by a low-pass filter at 10 Hz and a high-pass filter at 500 Hz. Surface electrodes were placed bilaterally in a bipolar configuration over six muscles—gluteus maximus (GMAX), rectus femoris (RF), biceps femoris (BF), lateral gastrocnemius medialis (GAS), soleus (SOL) and tibialis anterior (TA). Before placing the electrodes, the body hair was shaved and then the corresponding area was polished with sandpaper and alcohol cotton balls. When placing the transmitters, it was important to notice the interference with the wearable device and overlap with corresponding antagonistic muscles to avoid large measurement errors. All manipulations were performed by experts that specialized in surface EMG measurements. The calf was wrapped with knee-length stockings and the thigh was covered with textiles to prevent the transmitters from being thrown off at fast speeds.

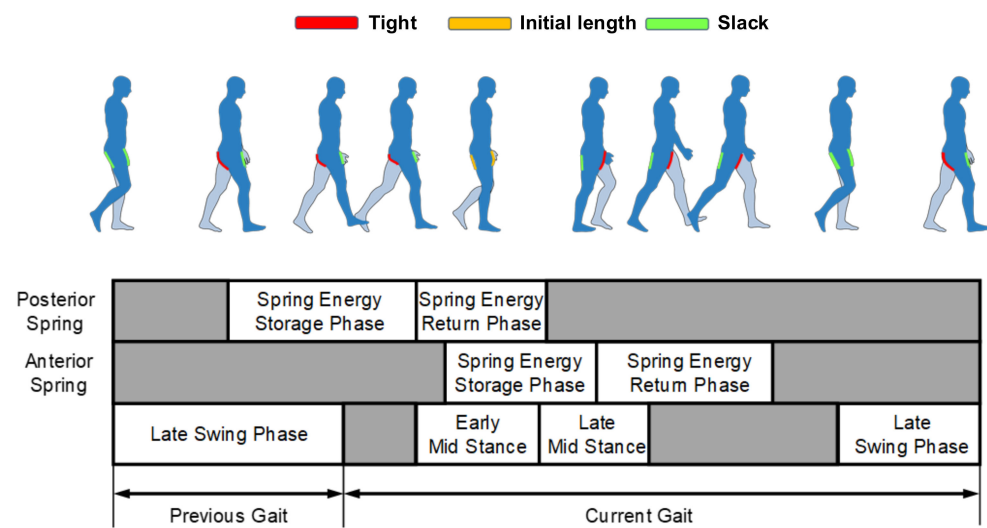


**Figure 3.** Schematic overview of the functional phases of passive springs located anteriorly and posteriorly across the hip joint in the gait cycle. This begins from the late swing phase in the previous gait to the end of the current gait. Green represents that the spring is slack, yellow represents the initial length of the spring (the spring is pretensioned by 1.5 cm) and red represents that the spring is tight.



**Figure 4.** (a) Front, (b) side and (c) rear view of a participant and the placement of electrical electrodes.

Walking kinematics were measured by a motion capture system (QTM, Qualysis, Gothenburg, Sweden) with sixteen lenses (OQUS500&OQUS700, Qualysis, Gothenburg, Sweden) at 300 Hz, tracking a set of 36 reflective markers (Figure 5). Markers were placed symmetrically on both sides of the anterior and posterior iliac muscles, the medial lateral condyle of knee joints, the inner and outer ankles, the heel, the first, second and fifth metatarsal bones, the thighs and the calves. The ground reaction forces (GRFs) and center of pressure (COP) were measured by a force plate (Kistler 9287C, Kistler, Winterthur, Switzerland) at 1000 Hz, which was connected to a computer through an amplifier and a data acquisition system. The physical parameters and pendulum equivalent lengths were measured and calculated according to the previous study [37].

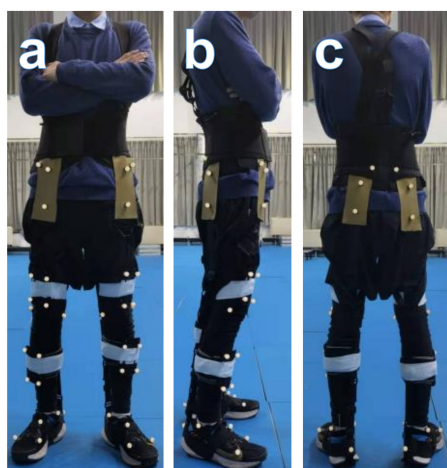


**Figure 5.** (a) Front, (b) side and (c) rear of a participant and the placement of markers.

### 2.3. Experimental Protocol

Before the formal experiment, a pre-experiment was conducted to evaluate the rationality of and familiarity with the experimental procedure. The frequencies in the previous study were: preferred frequency,  $\pm 15$ ,  $\pm 25$  and  $\pm 35\%$ , but it was found to be difficult to reach  $\pm 15\%$ , especially at lower frequencies during assisted walking, so the frequencies were set as preferred and  $\pm 10\%$ . In addition, participants performed a preferred speed selection session trial at 4.1, 4.3, 4.5, 4.7, 4.9 and 5.1 km/h (90 s at each speed, higher speeds were eliminated for an obvious increase of oxygen consumption during tests) to decide their preferred speed without exoskeleton assistance. Results showed that 6 out of 7 participants chose 4.5 km/h (1.25 m/s), and only 1 participant chose 4.3 km/h (1.19 m/s). The metabolic rates per distance at these two speeds of the participant who chose 4.3 km/h are almost the same. What is more, there was no statistical significance of differences between the measured step frequencies and the calculated frequencies through paired *t*-test. Based on this, the preferred speed without exoskeleton assistance (normal condition) was set as 1.25 m/s (general speed  $V_0$ ) in order to simplify the experimental setup slightly.

The experiment consists of three sessions: a familiarization session, a speed selection session and a walking session. In the familiarization session, participants performed an adaptive walking and speed selection protocol; the cardiopulmonary function parameters were also recorded at the same time.

During the speed selection session, a 4-min standing trial was performed at the beginning to collect baseline metabolic power. Then, the participants performed a 15-min speed selection trial at 4.3, 4.7, 5.1, 5.5, 5.9 and 6.3 km/h (90 s at each speed) to decide the preferred speed with assistance. Participants were asked to select a speed that made them feel both comfortable and obviously assisted by the device with the help of rating of perceived exertion (RPE). During the speed-selection trial, participants did not know the real time speed and when the subjects had directed the experimenter to the same speed on two consecutive occasions, it was deemed that this speed was the preferred speed  $V_1$ .

The walking session was divided into four conditions: walking at 1.25 m/s without assistance (normal condition) and with assistance (general condition) and walking at preferred speed with assistance (preferred condition) and without assistance (comparison condition). The normal condition represents the free walk under the preferred speed 1.25 m/s. The general condition represents walking with assistance without considering the changes (1.25 m/s) in preferred speed. The preferred condition represents walking with assistance when taking the changes of preferred speeds into consideration. The comparison condition represents the free walk without assistance at the preferred speed of the preferred condition. Sufficient rest intervals were set between every session to eliminate the effect of fatigue.

The treadmill speed was set at the self-selected speed constantly under the same condition in the walking session. At the beginning of a walking session, participants walked on the treadmill under their preferred gait features. The preferred frequency was obtained from the gait cycle duration, calculated by recording 20 steps. Then, participants walked for a 4-min trial following the metronome with  $\pm 10\%$  of the preferred step frequency, respectively. Procedures were the same in conditions of walking at 1.25 m/s with and without assistance. The trial for walking at the preferred assisted speed without the device was only performed once at its preferred step frequency as the comparison condition.

As the treadmill is only in the laboratory for measuring the oxygen consumption rather than the laboratory for collecting kinematic and kinetic data, the following method was used to reproduce walking on a treadmill when collecting kinematic and kinetic data. Step lengths were calculated in advance according to the data of the walking session, and simulated by markers placed on the floor. Participants walked under different walking conditions, following the markers and metronome in order to simulate the treadmill speed. Although the difference between walking on a flat ground and walking on a treadmill is unavoidable, the limitations of the equipment can only be offset through extra effort during the experiment. However, since the kinematic parameters only play a limited role in this article and the experimental condition is the same for every participant, the results obtained are still convincing.

#### 2.4. Participants

Seven healthy adults (age:  $23 \pm 0.93$ , height:  $172.43 \pm 1.92$  cm, weight:  $62.26 \pm 4.30$  kg) were recruited in the experiments and all of them gave their informed consent before participating. The sample size was chosen based on the previous research [38]. The study and protocol were approved by the Biomedical Ethics Committee of Hebei University of Technology and all experiments were performed in accordance with the relevant guidelines and regulations. Informed consent was obtained from each participant. Detailed information on participants' anthropometric measurements is shown in Table 1.

**Table 1.** Anthropometric measurements of the participants and equivalent pendulum length (mean and standard deviation).

	Right Thigh	Right Shank	Right Foot	Equivalent Pendulum Length
Length (m)	$0.42 \pm 0.02$	$0.36 \pm 0.03$	$0.13 \pm 0.01$	$0.55 \pm 0.02$
Mass (kg)	$6.24 \pm 0.44$	$2.90 \pm 0.22$	$0.91 \pm 0.06$	-

#### 2.5. Data Processing

The added mass of wearable devices was considered negligible with respect to the inertial and gravitational effects on participants' walking. The EMG raw data were first filtered with a 10 Hz high pass filter and a 500 Hz low pass filter. The filtered EMG signals were then rectified and smoothed by calculating the root mean square for a 50 ms moving window. The total activity of each muscle was calculated as the area under this curve for every group of 20 steps in the last 2 min of each 4-min trial.

The total EMG activity of a single muscle for each trial was normalized through dividing it by the total EMG activity of the preferred frequency, and the percentage of activity compared to walking at the preferred frequency was obtained by multiplying these normalized values by 100. The same normalization procedure was performed for  $V_{O_2}$ .

The carbon dioxide and oxygen rates were averaged across the last 2 min of each walking condition. Metabolic cost was calculated by using the regression equation of Zuntz

based on the thermal equivalent of O<sub>2</sub> for the nonprotein respiratory equivalent [39,40], as in Equation (1):

$$\text{metabolic cost (kcal/min)} = \dot{V}_{\text{O}_2} \times (1.2341 \times \text{RER} + 3.8124) \quad (1)$$

where RER is the respiratory exchange ratio. Then, the net metabolic rate per unit distance per unit body mass was calculated, as in Equation (2):

$$\frac{P_{\text{walk}} - P_{\text{stand}}}{v} \quad (2)$$

where  $P_{\text{walk}}$  and  $P_{\text{stand}}$  are the metabolic rate for walking and standing, respectively, and  $v$  is the preferred speed under different conditions.

### 2.6. Statistical Analysis

Wilcoxon test was used for the statistical significance of differences between general speed and preferred speed, as the general speed does not obey a normal distribution. The statistical significance of differences across step frequencies, step lengths, maximum hip angles, maximum plantarflexion angles and maximum dorsiflexion angles was tested using two-way analysis of variance (ANOVA). As VO<sub>2</sub> and muscle activity were normalized to the value obtained for walking at the preferred stride frequency, one-sample *t*-tests were used to determine the statistical significance of differences of the values between the preferred frequency condition and other conditions. The correlation between the duration of the single support phase and the duration of the gait cycle was also calculated to evaluate the level of participants utilizing the resonance of walking through the square of Pearson's linear correlation coefficient. Since the walking conditions rather than specific parameters were regarded as the variable when evaluating the walking efficiency, one-way analysis of variance (ANOVA) was used to detect the differences across the range of angles and the net metabolic rate per distance under different walking conditions. If a significant effect was found in one-way ANOVA, the Tukey's honestly significant difference (Tukey HSD) test will be used to compare pairs of conditions. A significance level of  $\alpha = 0.05$  was used for ANOVA, one-sample *t*-test Tukey HSD test and Wilcoxon test.

## 3. Results

### 3.1. Preferred Gait Features

Four different conditions were evaluated in this study: (1) normal condition: walking at 1.25 m/s without assistance; (2) preferred condition: walking at preferred speed with assistance; (3) general condition: walking at 1.25 m/s with assistance; (4) comparison condition: walking at preferred speed as that mentioned in (3) without assistance.

Exoskeleton assistance is able to substantially increase the self-selected speed (Wilcoxon test,  $p = 0.011 < 0.05$ ). In the speed selection trial, six participants chose 5.5 km/h (1.53 m/s), while one participant chose 5.1 km/h (1.41 m/s), 22.4% and 12.8% higher, respectively, compared to 1.25 m/s (Figure 6).

The frequency and step length were both significantly affected by the speed (ANOVA,  $p = 1.51 \times 10^{-4} < 0.05$ ,  $p = 2.15 \times 10^{-8} < 0.05$ ) (Figure 7). The preferred frequency of the preferred condition was higher than that of the normal condition and general condition by 9.2% and 6.8%, respectively, and frequency increased by 1.7% compared with the comparison condition. Similarly, the step length of the preferred condition was increased by 11.11% and 13.5% compared to the normal condition and general condition.

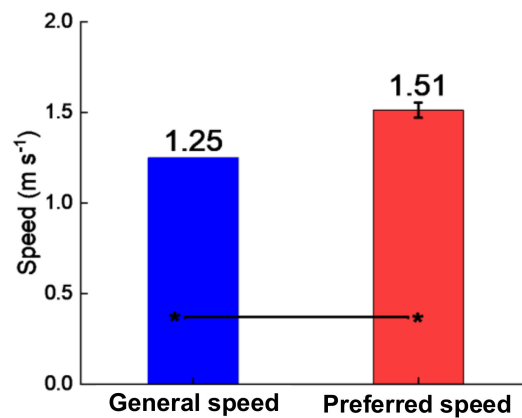


**Figure 6.** Mean (bars) and standard deviation (whiskers) of preferred walking speed under the normal and preferred condition (general speed and preferred speed); lines with asterisks denote statistically significant differences (Wilcoxon test,  $\alpha = 0.05$ ).

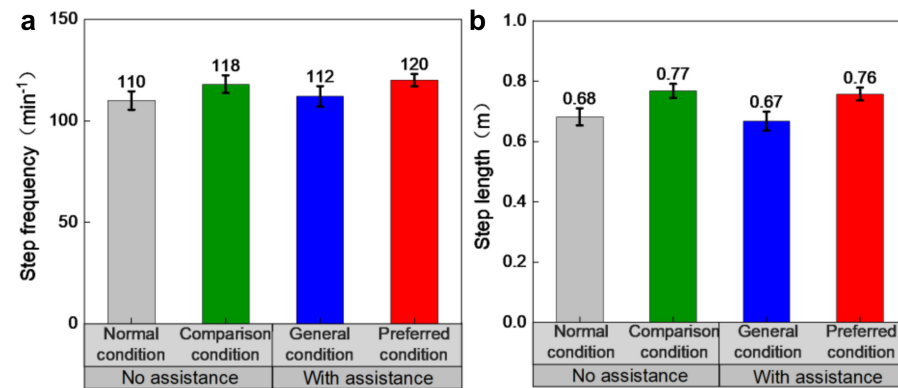


**Figure 7.** Preferred step frequency and step length under different conditions; (a) mean (bars) and standard deviation (whiskers) of step frequency under the normal condition (light grey bars), general condition (blue bars), preferred condition (red bars) and comparison condition (green bars); (b) mean (bars) and standard deviation (whiskers) of step length under the normal condition (light grey bars), general condition (blue bars), preferred condition (red bars) and comparison condition (green bars).

Mean joint angles and stick figures are shown to give a direct view of gaits under different conditions (Figure 8). Maximum plantarflexion and dorsiflexion angles were significantly affected by the exoskeleton assistance (ANOVA,  $p = 0.01 < 0.05$ ,  $p = 0.02 < 0.05$ ), as shown in Figure 9. The ranges of ankle, knee and hip angles are shown in Table 2. No significant differences were found in ranges of joint angles between different walking conditions.

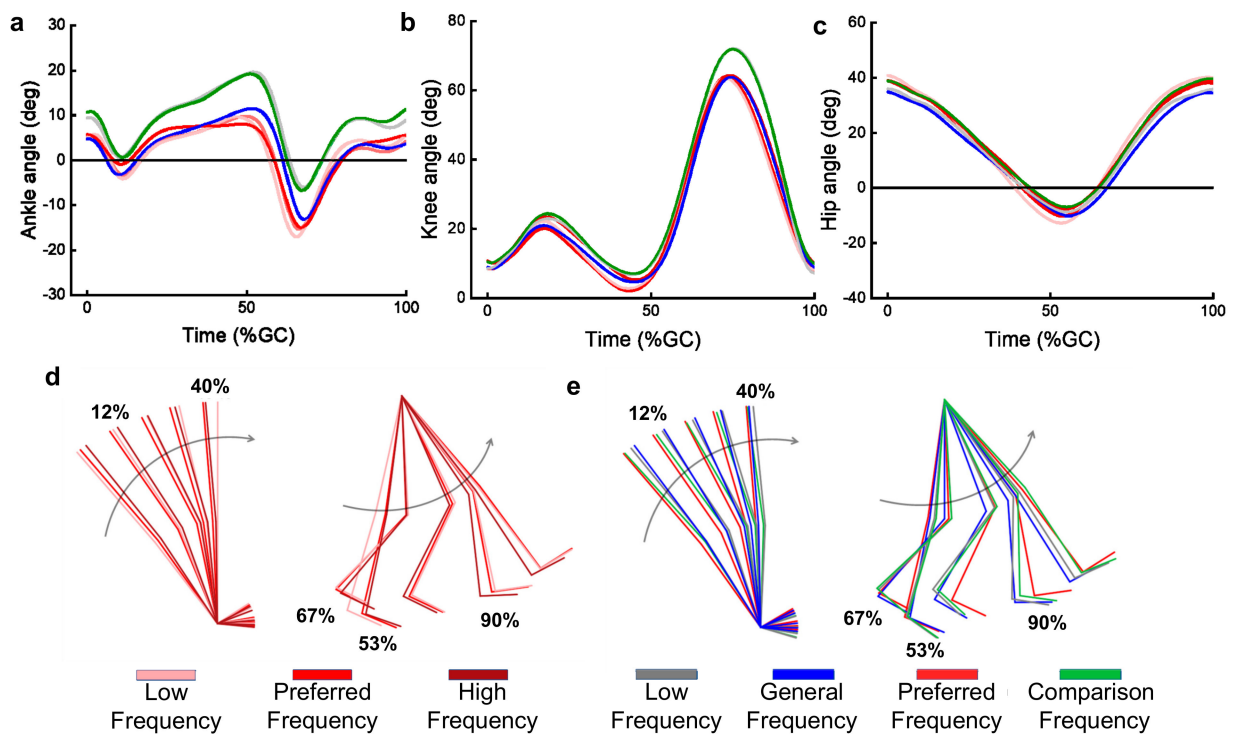


**Figure 8.** (a) Mean ankle angles under different walking conditions; (b) mean knee angles under different walking conditions; (c) mean hip angles under different walking conditions. (d) Stick figures of the mean walking kinematics at different frequencies under preferred speeds. Light red sticks depict walking at lower frequency, red sticks depict walking at preferred frequency and dark red sticks depict walking at higher frequency. Percentages represent different periods of the gait cycle. (e) Stick figures of the mean walking kinematics under different conditions. Light grey sticks depict walking under the normal condition, blue sticks depict walking under the general condition, red sticks depict walking under the preferred condition and green sticks depict walking under the comparison condition. Percentages represent different periods of the gait cycle.

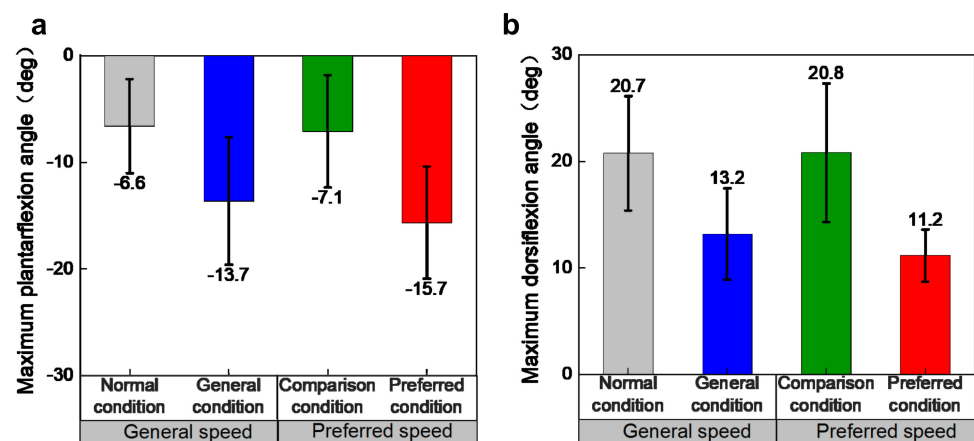


**Figure 9.** Ankle joint angles under different conditions; (a) mean (bars) and standard deviation (whiskers) of maximum plantarflexion angles under the normal condition (light grey bars), general condition (blue bars), preferred condition (red bars) and comparison condition (green bars); (b) mean (bars) and standard deviation (whiskers) of maximum dorsiflexion angles under the normal condition (light grey bars), general condition (blue bars), preferred condition (red bars) and comparison condition (green bars).

**Table 2.** The range of ankle, knee and hip angles under different walking conditions (mean and standard deviation).

	Normal Condition	General Condition	Preferred Condition	Comparison Condition
Ankle angle (deg)	27.34 ± 4.29	26.80 ± 3.76	26.80 ± 3.35	27.88 ± 4.71
Knee angle (deg)	66.28 ± 3.98	61.38 ± 6.15	63.63 ± 4.71	66.22 ± 4.22
Hip angle (deg)	49.63 ± 9.46	50.02 ± 7.27	53.04 ± 6.25	50.86 ± 9.32

### 3.2. Resonant Walking

Under the general condition (Figure 10a), only 2 of the 7 participants had the least oxygen consumption at the preferred frequency, and the oxygen consumption was only a little better modeled as a quadratic function of  $\Delta\omega$  ( $R^2 = 0.18$ ,  $p = 0.167$ ) than a linear function ( $R^2 = 0.114$ ,  $p = 0.134$ ). As in the preferred condition (Figure 10b), the oxygen consumption is the lowest at the preferred frequency among all participants under the preferred condition, and the oxygen consumption was best modeled as a quadratic function of  $\Delta\omega$  ( $R^2 = 0.236$ ,  $p = 0.089$ ) over a linear function ( $R^2 = 0.05$ ,  $p = 0.328$ ). There is still a significant trend on the quadratic curve fitting although the fitting degree is not as expected. The oxygen consumption at preferred frequency under the preferred condition was significantly different from lower frequency (One sample  $t$ -test,  $p = 0.004 < 0.05$ ) and higher frequency (One sample  $t$ -test,  $p = 0.011 < 0.05$ ). The preferred frequency under the general condition was not significantly different from lower frequency (One sample  $t$ -test,  $p = 0.081$ ), but was from higher frequency (One sample  $t$ -test,  $p = 0.016$ ).

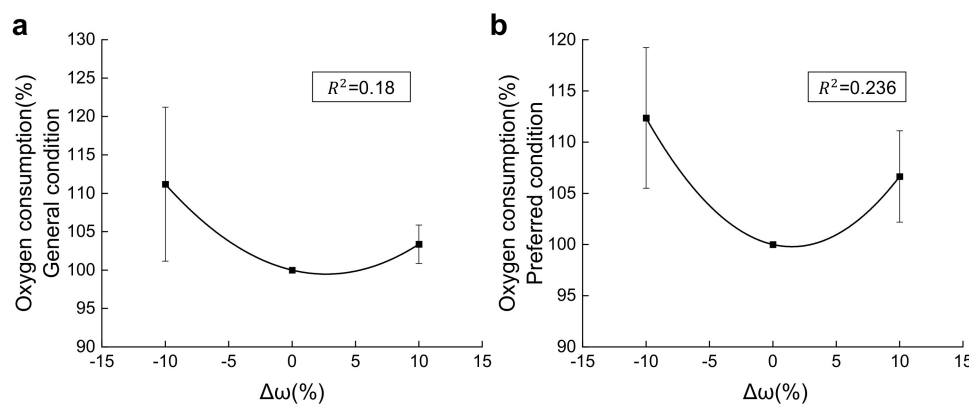


**Figure 10.** Mean and standard deviation of oxygen consumption (as a percentage of the value for walking at the preferred frequency) for the last two minutes of walking across the three different step frequency conditions. The step frequencies are plotted as the percentage difference from the preferred frequency,  $\Delta\omega$ . The preferred step frequency is  $\Delta\omega = 0\%$ . The solid line represents the quadratic curve with error bars of standard deviation. Each subplot is a different condition: (a) general condition; (b) preferred condition.

Under the general condition (Figure 11), the EMG of all muscles was modeled just a little more accurately as a quadratic function of  $\Delta\omega$  ( $R^2$  ranging from 0.041 to 0.375) than linear function ( $R^2$  ranging from 0.16 to 0.272). The EMG of TA, GAS at preferred frequency is significantly different from lower frequencies, while the EMG of RF at preferred frequency is significantly different from higher frequencies. The EMG of SOL, GM and BF at preferred frequency showed no significant difference with either lower or higher frequencies.

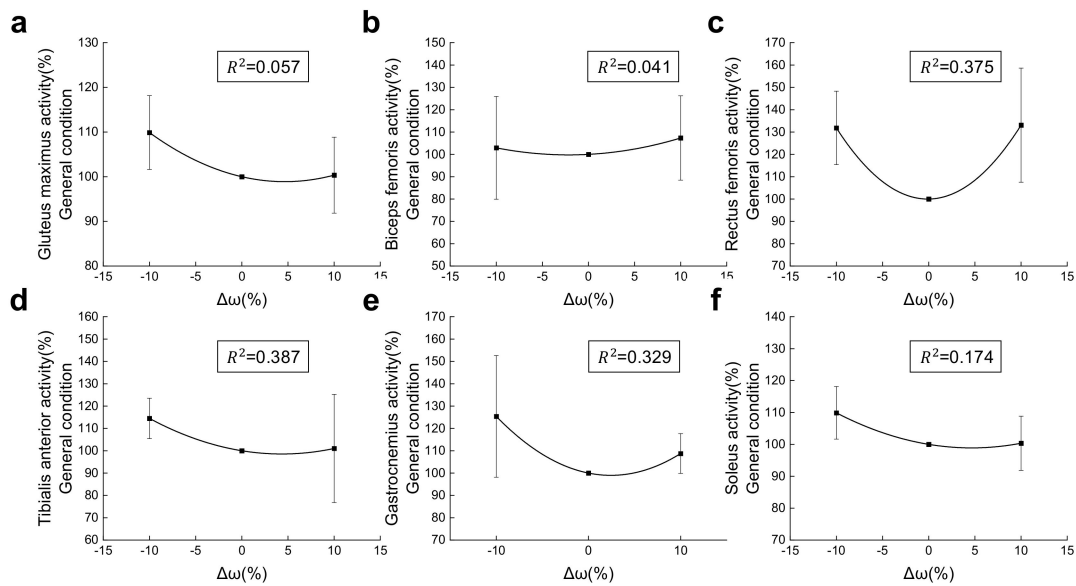


**Figure 11.** Mean and standard deviation of the muscle activity (as a percentage of the value for walking at the preferred step frequency) for the last two minutes of walking across the three different frequencies under the general condition. Step frequencies are plotted as the percentage difference from the preferred frequency,  $\Delta\omega$ . The preferred frequency is  $\Delta\omega = 0\%$ . The solid line represents the quadratic curve with error bars of standard deviation. Each subplot is a different muscle under the general condition: (a) gastrocnemius muscle; (b) biceps femoris muscle; (c) rectus femoris muscle; (d) tibialis anterior muscle; (e) gastrocnemius muscle; (f) soleus muscle.

Under the preferred condition (Figure 12), the EMG of all muscles was best modeled as a quadratic function of  $\Delta\omega$  ( $R^2$  ranging from 0.407 to 0.865) over a linear function ( $R^2$  ranging from 0.005 to 0.064). The EMG of TA, GAS, SOL, GM, BF and RF at preferred frequency is significantly different from both lower and higher frequencies. Detailed information on modeling and statistical significance analysis under the preferred and general condition is shown in Tables 3 and 4.

The correlation between the duration of the single support phase and the period of the natural frequency of the spring–mass model under the preferred condition ( $R^2 = 0.7$ ) was better than under the general condition ( $R^2 = 0.57$ ), as shown in Figure 13.

**Table 3.** Results of modeling analysis for muscle activity and oxygen consumption and the differences between values at the preferred and other frequencies under general condition.

		VO <sub>2</sub>	TA	GAS	SOL	GM	BF	RF
R <sup>2</sup>	Linear	0.134	0.272	0.135	0.124	0.042	0.016	0.236
	Quadratic	0.167	0.387	0.329	0.174	0.057	0.041	0.375
p	With lower frequency	0.081	0.025	0.037	0.182	0.286	0.774	0.600
	With higher frequency	0.016	0.808	0.106	0.856	0.979	0.216	0.018

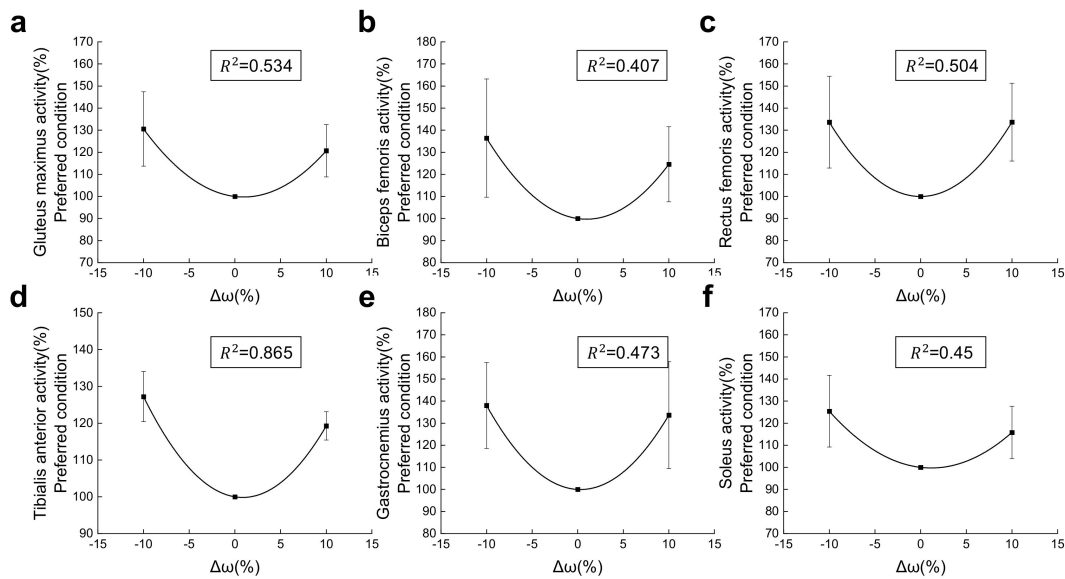


**Figure 12.** Mean and standard deviation of the muscle activity (as a percentage of the value for walking at the preferred step frequency) for the last two minutes of walking across the three different frequencies under the preferred condition. Step frequencies are plotted as the percentage difference from the preferred frequency,  $\Delta\omega$ . The preferred frequency is  $\Delta\omega = 0\%$ . The solid line represents the quadratic curve with error bars of standard deviation. Each subplot is a different muscle under the preferred condition: (a) gastrocnemius muscle; (b) biceps femoris muscle; (c) rectus femoris muscle; (d) tibialis anterior muscle; (e) gastrocnemius muscle; (f) soleus muscle.

**Table 4.** Results of modeling analysis for muscle activity and oxygen consumption and the differences between values at the preferred and other frequencies under preferred condition.

		VO <sub>2</sub>	TA	GAS	SOL	GM	BF	RF
R <sup>2</sup>	Linear	0.089	0.070	0.005	0.064	0.054	0.041	$6.13 \times 10^{-7}$
	Quadratic	0.328	0.865	0.473	0.450	0.534	0.407	0.504
p	With lower frequency	0.004	$6.6 \times 10^{-5}$	0.003	0.009	0.004	0.016	0.007
	With higher frequency	0.011	$1.8 \times 10^{-5}$	0.014	0.017	0.005	0.012	0.003

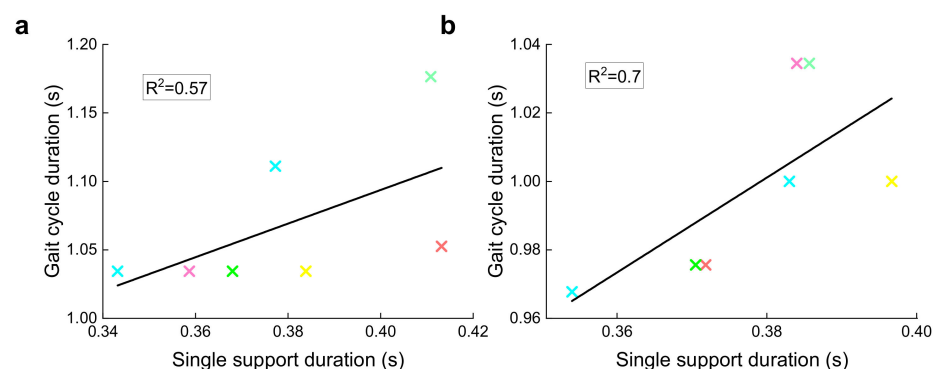


**Figure 13.** Correlation between the duration of the single support phase and the period of the gait cycle; (a) general condition; (b) preferred condition. The single support duration was more closely related to the natural frequency of the hybrid spring-mass model under the preferred condition rather than the general condition.

### 3.3. Net Metabolic Rate

The effects of walking on net metabolic rate varied widely among participants (Figures 14 and 15). Compared with the normal condition, the net metabolic rate changes under the general condition ranged from a 0.59% reduction to a 22.25% increase, with an average increase of 11.62%. Only 1 participant had a reduction in net metabolic rate under the general condition. In the preferred condition, the metabolic rate was reduced by 4.53% compared with the general condition. In total, 4 of 7 participants had a reduction in metabolic rate, 2 of which were reduced by 17.18% and 16.18%; the others were reduced by 5.42% and 7.65%, respectively. The net metabolic rate of the remaining participants increased from 1.57% to 7.52%. Compared with the comparison condition, 6 participants' net metabolic rates decreased, the highest reduction being 16.92%; however, the remaining participants' rates did not decrease by more than 10%. Only 1 participant had an increase in net metabolic rate. There was no significant difference in net metabolic rate between conditions.

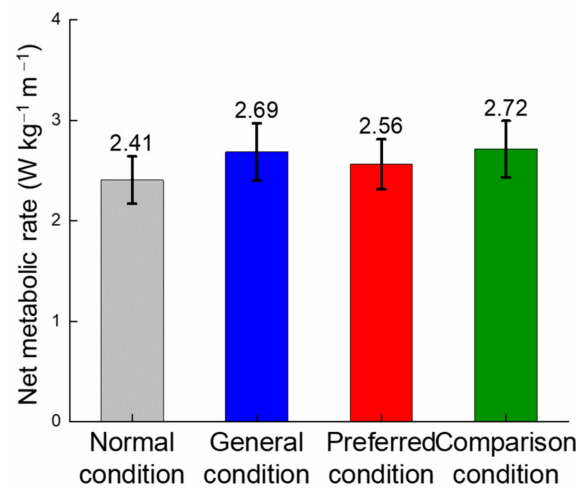


**Figure 14.** Mean (bars) and standard deviation (whiskers) of the net metabolic rate measured during walking under the normal condition (light grey), general condition (blue), preferred condition (red) and comparison condition (green).

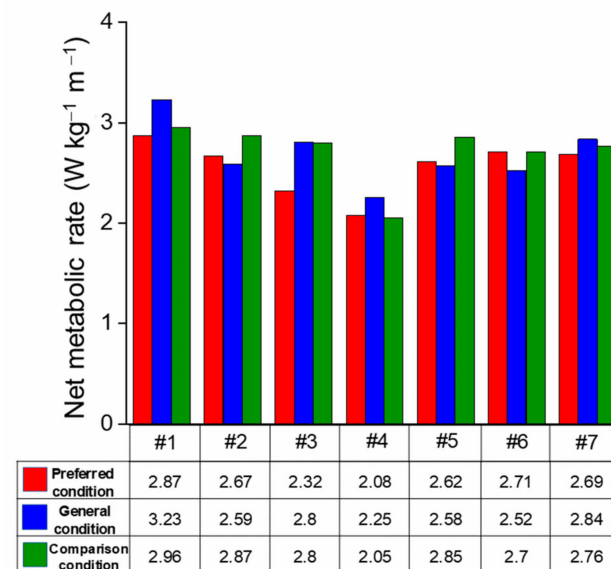


**Figure 15.** Net metabolic power for each participant under the preferred (red), general (blue) and comparison (green) condition; the table shows the specific values of net metabolic rate.

#### 4. Discussion

Exoskeleton assistance was found to substantially increase the preferred walking speed. The speed selection session induced participants to walk 0.26 m/s (21%) faster. This is an obvious increase in speed, but not as large as in the previous study of Collins (around 50% of the speed increase of Collins). This is mainly because the assistance device used in this study is unpowered and has effects on multiple joints; a huge increase of speed would cause a corresponding increase in the cost for transportation, as the device should be actuated by users, which is unreasonable behavior for walking efficiency in a subjective perspective. In addition, the formal and pre-experiments showed that the speed of the most comfortable RPE value increased and the RER decreased after several sessions, indicating that the assistance devices have large potential for speed improvement. These results demonstrate that, with appropriate training, unpowered exoskeletons can induce people to walk at faster speeds.

Speed has great effect on the step frequency and step length, and significantly improves them under the same assistance condition. There were only negligible differences between different assistance conditions at the same speed. However, it is still possible that there is a complicated relationship between the exoskeleton assistance and the step frequency and length, as the corresponding changes in preferred gait features are related to the increased speed that is caused by the assistance. Effects of the exoskeleton on the ankle joint angle lasted throughout the gait cycle, especially during the plantarflexion and dorsiflexion phases, and the exoskeleton significantly decreased the dorsiflexion angle and increased the plantarflexion angle. However, the effect on knee and hip angles was not significant, only during the swing phase there was more flexion of the knee angle under assistance. There was no significant difference in the angular range of all the lower extremity joints under different walking conditions. Especially for the ankle joint angle, although the maximum plantarflexion and dorsiflexion angles changed due to the assistance of the exoskeleton, these curves were almost only translated up and down. These results suggested that there were no obvious changes in walking features. These results demonstrated that the effect of exoskeleton on walking kinematics is limited and did not significantly alter walking habits.

In agreement with previous research [25], the preferred step frequency utilizes the least oxygen compared with higher or lower step frequencies, and significant difference between the preferred frequency and others occurred under the preferred condition. As the primary source of metabolic cost in walking, muscles have been proven to have the lowest activity at preferred frequency at a constant speed. In this study, GM, SOL, GAS, TA, BF and RF muscles are minimally activated at the preferred frequency just as in previous reports [25]. As there was a more accurate result from quadratic fitting rather than in linear fitting, it is believed that the resonance did occur during the assisted walking under the preferred condition. However, for the general condition, there was no significant difference between the  $R^2$  of quadratic fitting and linear fitting. This could be the evidence that stable-resonant walking did not exist under the general condition. Yet, there is still a possibility that the adjustment time under the general condition is not enough in this experiment, since the correlation between the single support duration and gait cycle duration is 0.57. This may be the explanation of the above results under the general condition, but some unclear problems still remain. As the lower and higher frequencies are set as  $\pm 10\%$  of preferred frequency, it is possible that the small gap and small quantities of frequencies are the main reason for the small difference between the  $R^2$  of the quadratic and linear fitting under the general condition. Moreover, participants had to adjust their cadences in order to coordinate with the metronome, which would impact the breath and EMG during walking. As a result, whether resonant walking did exist under the general condition remains unclear. Unlike in previous studies [25], the muscle activity of BF and RF was higher in lower frequencies with respect to higher frequencies; this may be due to there being more effort conducted in lower frequencies to actuate the device.

A higher correlation between the single support duration and gait cycle duration was shown under the preferred condition ( $R^2 = 0.7$ ) compared to the general condition

( $R^2 = 0.57$ ), indicating a higher degree of resonance utilization [30]. Walking is more sensitive to resonance under the preferred speed with the exoskeleton. As a result, the proper exoskeleton design and movement parameters will lead to a condition that is much closer to the resonance, thus benefiting the walking efficiency.

Unexpectedly, the net metabolic rate under the general condition showed a totally different result insofar as only one participant had a reduction of 0.59%. Since the gait feature is almost the same, the increase between the normal and general condition can be explained by the device's characteristics such as unpowered and multi-joint-assisted. On the contrary, the net metabolic rate of the preferred condition showed a positive effect on energy saving, with 6 of 7 participants having a reduction on their net metabolic rates compared to the comparison condition. The difference between these two trends suggested the great effect of preferred speeds on assisting results. In addition, a 4.53% reduction was found between the preferred and general condition; 4 of 7 participants under the preferred condition showed a reduction in net metabolic rate with respect to the general condition. The increased net metabolic rate of the general condition is similar to the result in [41] (which had a 23% higher metabolic increase compared to walking without exoskeletons when using the exoskeleton with energy stored from knee extension and released for ankle plantarflexion); this could be explained by the assistance for the whole lower body. As this assistance has a great influence on assisted walking, new gait features will be required to improve the overall walking efficiency. Considering the increase of the net metabolic rate between the normal and general condition, it is believed that the reduction between the preferred and general condition can be explained by the resonant walking. This could be verified by the correlation between the duration of the single support phase and the period of the gait cycle. The higher correlation ( $R^2 = 0.7$  for the preferred condition and  $R^2 = 0.57$  for the general condition) of the preferred condition indicates that walking under the preferred condition utilizes the resonance of the whole body more efficiently.

The results of this study showed the important impact of resonant walking on exoskeleton devices, especially on unpowered exoskeletons. Preferred speed changed after assistance. When having a greater impact on walking, exoskeletons will also bring greater constraints. If resonant walking cannot be fully utilized, negative results may appear, just as in the general condition in this study. As a result, it is necessary to take the change of gait features into consideration during the design and evaluation of exoskeletons for global and further optimization of assisted walking. As is related to the preferred speed, the introduced concept of resonant walking is able to explain the U-shaped stiffness-metabolic rate curve and the lowest energy consumption at moderate stiffness. What is more, the personalized design is the key to solving the problem of the widely varied metabolic rate. Owing to the close relationship with body parameters, resonant walking is the most representative characteristic of human movement; hence it will certainly make a great contribution to the personalized design of exoskeletons.

Certainly, there are still some limitations of the research. First, the preferred speed could only be closely obtained in the speed-selection session because of the limitation of the treadmill, and this would have some unstable effects when evaluating the resonance condition of walking. Second, muscle activity and energy consumption are only two aspects that affect resonant walking; other aspects such as stability were not evaluated in this research, but muscle activity and oxygen consumption are the only evidence to verify resonant walking in this article, so it is not that comprehensive. More evidence that can prove resonant walking should be considered in a further study. Finally, the reduced number of participants is also a limitation that cannot be ignored, because this may influence the results of statistical analysis. Further studies about assistance performance under different speeds and spring stiffness should be conducted to map out the complicated relationship between exoskeleton assistance and resonant walking, which is consistent with the previous study [42]. In addition, in order to better study resonance in assisted walking, models that are capable of clearly describing resonant walking should be established. The

complex relationship between preferred speed, exoskeleton stiffness and body parameters should be delineated in the future study.

## 5. Conclusions

In this article, the effect of exoskeleton assistance on preferred speeds was tested. Resonant walking was proven to exist in assisted walking, and the higher utilization of resonance with exoskeleton assistance led to lower energy consumption. The relationship of the body parameters, the spring stiffness and corresponding preferred gait features should be the subject of further research in the future. It is believed that changes in preferred speeds should be taken into consideration in further studies, and resonant walking will play an important role in the design and evaluation of unpowered soft exoskeletons.

**Author Contributions:** Conceptualization, H.W.; methodology, H.W.; software, H.W.; validation, H.W., J.W., Q.T. and Y.Z.; formal analysis, H.W.; resources, Z.Z. and S.G.; data curation, H.W., Z.Z., J.W., Q.T. and Y.Z.; writing—original draft preparation, H.W.; writing—review and editing, S.G. All authors have read and agreed to the published version of the manuscript.

**Funding:** This research was funded by the National Key Research and Development Program of China under Grant 2019YFB1312500.

**Institutional Review Board Statement:** The study was conducted in accordance with the Declaration of Helsinki, and approved by the Institutional Review Board of Biomedical Ethics Committee of Hebei University of Technology (NO. HEBUTHMEC2022020, 1 November 2021).

**Informed Consent Statement:** Informed consent was obtained for all subjects involved in the study.

**Data Availability Statement:** The datasets used and/or analyzed during the current study are available from the corresponding author on reasonable request. Due to the current situation influenced by COVID-19, some portion of the raw data that are stored in Tianjin University of Sport cannot be integrated right now, so we decided to manage the raw data by ourselves and the data are available from the corresponding author Z.Z. (zzy@hebut.edu.cn) upon reasonable request.

**Conflicts of Interest:** The authors declare no conflict of interest.

## References

1. Li, Y.; Sun, H.; Wang, C. Key Technologies of Lower Limb Power-Assisted Exoskeleton Robots: A Review. In Proceedings of the 2021 6th International Conference on Control, Robotics and Cybernetics (CRC), Shanghai, China, 9–11 October 2021; pp. 25–31.
2. Rodríguez-Fernández, A.; Lobo-Prat, J.; Font-Llagunes, J.M. Systematic review on wearable lower-limb exoskeletons for gait training in neuromuscular impairments. *J. Neuroeng. Rehabil.* **2021**, *18*, 22–43. [[CrossRef](#)] [[PubMed](#)]
3. Proud, J.K.; Lai, D.T.; Mudie, K.L.; Carstairs, G.L.; Billing, D.C.; Garofolini, A.; Begg, R.K. Exoskeleton application to military manual handling tasks. *Hum. Factors* **2022**, *64*, 527–554. [[CrossRef](#)] [[PubMed](#)]
4. Leclair, J.; Pardoel, S.; Helal, A.; Doumit, M. Development of an unpowered ankle exoskeleton for walking assist. *Disabil. Rehabil. Assist. Technol.* **2018**, *15*, 1–13. [[CrossRef](#)] [[PubMed](#)]
5. Nasiri, R.; Ahmadi, A.; Ahmadabadi, A.A. Reducing the Energy Cost of Human Running Using an Unpowered Exoskeleton. *IEEE Trans. Neural Syst. Rehabil. Eng.* **2018**, *26*, 2026–2032. [[CrossRef](#)]
6. Wang, X.; Guo, S.; Qu, B.; Song, M.; Qu, H. Design of a Passive Gait-based Ankle-foot Exoskeleton with Self-adaptive Capability. *Chin. J. Mech. Eng.* **2020**, *33*, 49. [[CrossRef](#)]
7. Zhou, T.; Xiong, C.; Zhang, J.; Hu, D.; Chen, W.; Huang, X. Reducing the metabolic energy of walking and running using an unpowered hip exoskeleton. *Neuroeng. Rehabil.* **2021**, *18*, 95. [[CrossRef](#)]
8. Yandell, M.B.; Tacca, J.R.; Zelik, K.E. Design of a Low Profile, Unpowered Ankle Exoskeleton That Fits Under Clothes: Overcoming Practical Barriers to Widespread Societal Adoption. *IEEE Trans. Neural Syst. Rehabil. Eng.* **2019**, *27*, 712–723. [[CrossRef](#)]
9. Ishikawa, M.; Komi, P.V.; Grey, M.J.; Lepola, V.; Bruggemann, G.P. Muscle-tendon interaction and elastic energy usage in human walking. *J. Appl. Physiol.* **2005**, *99*, 603. [[CrossRef](#)]
10. Sawicki, G.S.; Lewis, C.L.; Ferris, D.P. It Pays to Have a Spring in Your Step. *Exerc. Sport Sci. Rev.* **2009**, *37*, 130–138. [[CrossRef](#)]
11. Zelik, K.E.; Kuo, A.D. Human walking isn't all hard work: Evidence of soft tissue contributions to energy dissipation and return. *J. Exp. Biol.* **2010**, *213*, 4257–4264. [[CrossRef](#)]
12. Collins, S.H.; Wiggin, M.B.; Sawicki, G.S. Reducing the energy cost of human walking using an unpowered exoskeleton. *Nature* **2015**, *522*, 212–215. [[CrossRef](#)]
13. Dijk, W.V.; Kooij, H.; Hekman, E. A passive exoskeleton with artificial tendons: Design and experimental evaluation. In Proceedings of the IEEE International Conference on Rehabilitation Robotics, Zurich, Switzerland, 27 June–1 July 2011; pp. 1–6.

14. Haufe, F.L.; Wolf, P.; Riener, R.; Grimmer, M. Biomechanical Effects of Passive Hip Springs During Walking. *J. Biomech.* **2021**, *98*, 109432. [[CrossRef](#)]
15. Yang, J.; Park, J.; Kim, J.; Park, S.; Lee, G. Reducing the energy cost of running using a lightweight, low-profile elastic exosuit. *J. Neuroeng. Rehabil.* **2021**, *18*, 129–140. [[CrossRef](#)]
16. Panizzolo, F.A.; Annese, E.; Paoli, A.; Marcolin, G. A Single Assistive Profile Applied by a Passive Hip Flexion Device Can Reduce the Energy Cost of Walking in Older Adults. *Appl. Sci.* **2021**, *11*, 2851. [[CrossRef](#)]
17. Panizzolo, F.A.; Bolgiani, C.; Liddo, L.D.; Annese, E.; Marcolin, G. Reducing the energy cost of walking in older adults using a passive hip flexion device. *J. NeuroEng. Rehabil.* **2019**, *16*, 117. [[CrossRef](#)]
18. Xiong, C.; Zhou, T.; Zhou, L.; Wei, T.; Chen, W. Multi-articular passive exoskeleton for reducing the metabolic cost during human walking. In Proceedings of the Wearable Robotics Association Conference (WearRAcon), Phoenix, NJ, USA, 25–27 May 2019; pp. 63–67.
19. Zhou, T.; Xiong, C.; Zhang, J.; Zhang, J.; Chen, W.; Huang, X. Regulating Metabolic Energy Among Joints During Human Walking Using a Multiarticular Unpowered Exoskeleton. *IEEE Trans. Neural Syst. Rehabil. Eng.* **2021**, *29*, 662–672. [[CrossRef](#)]
20. Song, S.; Collins, S.H. Optimizing Exoskeleton Assistance for Faster Self-Selected Walking. *IEEE Trans. Neural Syst. Rehabil. Eng.* **2021**, *29*, 786–795. [[CrossRef](#)]
21. Zarrugh, M.Y.; Radcliffe, C.W. Predicting metabolic cost of level walking. *Eur. J. Appl. Physiol. Occup. Physiol.* **1978**, *38*, 215–223. [[CrossRef](#)]
22. Holt, K.G.; Hamill, J.; Andres, R.O. The force-driven harmonic oscillator as a model for human locomotion. *Hum. Mov. Sci.* **1990**, *9*, 55–68. [[CrossRef](#)]
23. Holt, K.G.; Hamill, J.; Andres, R.O. Predicting the minimal energy costs of human walking. *Med. Sci. Sports Exerc.* **1991**, *23*, 491–498. [[CrossRef](#)]
24. Holt, K.G.; Jeng, S.F.; Ratcliffe, R.; Hamill, J. Energy Cost and Stability During Human Walking at the Preferred Stride Frequency. *J. Mot. Behav.* **1996**, *27*, 164–178. [[CrossRef](#)]
25. Russell, D.M.; Haworth, J.L. Walking at the preferred stride frequency maximizes local dynamic stability of knee motion. *J. Biomech.* **2014**, *47*, 102–108. [[CrossRef](#)]
26. Obusek, J.P.; Holt, K.G.; Rosenstein, R.M. The hybrid mass-spring pendulum model of human leg swinging: Stiffness in the control of cycle period. *Biol. Cybern.* **1995**, *73*, 139–147. [[CrossRef](#)]
27. Fonseca, S.T.; Holt, K.G.; Saltzman, E.; Fetzters, L. A dynamical model of locomotion in spastic hemiplegic cerebral palsy: Influence of walking speed. *Clin. Biomech.* **2001**, *16*, 793–805. [[CrossRef](#)]
28. Holt, K.G.; Obusek, J.P.; Fonseca, S.T. Constraints on disordered locomotion A dynamical systems perspective on spastic cerebral palsy. *Hum. Mov. Sci.* **1996**, *15*, 177–202. [[CrossRef](#)]
29. Hartmut, G.; Andre, S.; Reinhard, B.; Blickhan, R. Compliant leg behaviour explains basic dynamics of walking and running. *Proc. R. Soc. B Biol. Sci.* **2006**, *273*, 2861–2867.
30. Kim, S.; Park, S. Leg stiffness increases with speed to modulate gait frequency and propulsion energy. *J. Biomech.* **2011**, *44*, 1253–1258. [[CrossRef](#)]
31. Kim, S.; Park, S. The oscillatory behavior of the CoM facilitates mechanical energy balance between push-off and heel strike. *J. Biomech.* **2012**, *45*, 326–333. [[CrossRef](#)]
32. Hong, H.; Kim, S.; Kim, C.; Kim, C.; Lee, S.; Park, S. Spring-like gait mechanics observed during walking in both young and older adults. *J. Biomech.* **2013**, *46*, 77–82. [[CrossRef](#)]
33. Lee, M.; Kim, S.; Park, S. Resonance-based oscillations could describe human gait mechanics under various loading conditions. *J. Biomech.* **2014**, *47*, 319–322. [[CrossRef](#)]
34. Ryu, H.X.; Park, S. Estimation of unmeasured ground reaction force data based on the oscillatory characteristics of the center of mass during human walking. *J. Biomech.* **2018**, *71*, 135–143. [[CrossRef](#)] [[PubMed](#)]
35. Kuo, A.D.; Collins, S.H. The six determinants of gait and the inverted pendulum analogy: A dynamic walking perspective. *Hum. Mov. Sci.* **2007**, *26*, 617–656. [[CrossRef](#)] [[PubMed](#)]
36. Collins, S.H.; Kuo, A.D. Recycling Energy to Restore Impaired Ankle Function during Human Walking. *PLoS ONE* **2010**, *5*, e9307. [[CrossRef](#)] [[PubMed](#)]
37. Vaughan, C.L.; Davis, B.L.; O'Connor, J.C. *Dynamics of Human Gait*, 2nd ed.; Hanover: Human Kinetics Pub: Western Cape, South Africa, 1992; pp. 15–22.
38. Malcolm, P.; Galle, S.; Derave, W.; Clercq, D.D. Bi-articular knee-ankle-foot exoskeleton produces higher metabolic cost reduction than weight-matched mono-articular exoskeleton. *Front. Neurosci.* **2018**, *12*, 69–82. [[CrossRef](#)]
39. Mcdaniel, J.; Durstine, J.L.; Hand, G.A. Determinants of metabolic cost during submaximal cycling. *J. Appl. Physiol.* **2002**, *93*, 823–828. [[CrossRef](#)]
40. Zuntz, N. Ueber die Bedeutung der verschiedenen Nährstoffe als Erzeuger der Muskelkraft. *Arch. Die Gesamte Physiol. Menschen Tiere* **1901**, *83*, 557–571. (In Germany) [[CrossRef](#)]
41. Etenzi, E.; Borzuola, R.; Grabowski, A.M. Passive-elastic knee-ankle exoskeleton reduces the metabolic cost of walking. *J. NeuroEng. Rehabil.* **2020**, *17*, 104. [[CrossRef](#)]
42. Nuckols, R.W.; Sawicki, G.S. Impact of elastic ankle exoskeleton stiffness on neuromechanics and energetics of human walking across multiple speeds. *J. NeuroEng. Rehabil.* **2020**, *17*, 75–93. [[CrossRef](#)]